

# Multiplicity of Galactic Cepheids from long-baseline interferometry – III. Sub-percent limits on the relative brightness of a close companion of $\delta$ Cephei

A. Gallenne,<sup>1</sup>★ A. Mérand,<sup>1</sup> P. Kervella,<sup>2,3</sup> J. D. Monnier,<sup>4</sup> G. H. Schaefer,<sup>5</sup>  
R. M. Roettenbacher,<sup>4</sup> W. Gieren,<sup>6</sup> G. Pietrzyński,<sup>6,7</sup> H. McAlister,<sup>5</sup>  
T. ten Brummelaar,<sup>5</sup> J. Sturmann,<sup>5</sup> L. Sturmann,<sup>5</sup> N. Turner<sup>5</sup> and R. I. Anderson<sup>8</sup>

<sup>1</sup>European Southern Observatory, Alonso de Córdova 3107, Casilla 19001, Santiago 19, Chile

<sup>2</sup>LESIA (UMR 8109), Observatoire de Paris, PSL, CNRS, UPMC, Univ. Paris-Diderot, 5 place Jules Janssen, F-92195 Meudon, France

<sup>3</sup>Unidad Mixta Internacional Franco-Chilena de Astronomía (CNRS UMI 3386), Departamento de Astronomía, Universidad de Chile, Camino El Observatorio 1515, Las Condes, Santiago, Chile

<sup>4</sup>Department of Astronomy, University of Michigan, 918 Dennison Building, Ann Arbor, MI 48109-1090, USA

<sup>5</sup>The CHARA Array of Georgia State University, Mount Wilson, CA 91023, USA

<sup>6</sup>Universidad de Concepción, Departamento de Astronomía, Casilla 160-C, Concepción, Chile

<sup>7</sup>Nicolaus Copernicus Astronomical Centre, Polish Academy of Sciences, Bartycka 18, PL-00-716 Warszawa, Poland

<sup>8</sup>Department of Physics and Astronomy, Johns Hopkins University, Baltimore, MD 21218, USA

Accepted 2016 June 3. Received 2016 June 2; in original form 2016 May 19

## ABSTRACT

We report new CHARA/Michigan InfraRed Combiner interferometric observations of the Cepheid archetype  $\delta$  Cep, which aimed at detecting the newly discovered spectroscopic companion. We reached a maximum dynamic range  $\Delta H = 6.4$ , 5.8 and 5.2 mag, respectively, within the relative distance to the Cepheid  $r < 25$  mas,  $25 < r < 50$  mas and  $50 < r < 100$  mas. Our observations did not show strong evidence of a companion. We have a marginal detection at  $3\sigma$  with a flux ratio of 0.21 per cent, but nothing convincing as we found other possible probable locations. We ruled out the presence of companion with a spectral type earlier than F0V, A1V and B9V, respectively for the previously cited ranges  $r$ . From our estimated sensitivity limits and the Cepheid light curve, we derived lower limit magnitudes in the  $H$  band for this possible companion to be  $H_{\text{comp}} > 9.15$ , 8.31 and 7.77 mag, respectively, for  $r < 25$  mas,  $25 < r < 50$  mas and  $50 < r < 100$  mas. We also found that to be consistent with the predicted orbital period (Anderson et al.), the companion has to be located at a projected separation  $< 24$  mas with a spectral type later than an F0V star.

**Key words:** techniques: high angular resolution – techniques: interferometric – binaries: close – stars: variables: Cepheids.

## 1 INTRODUCTION

$\delta$  Cep is well known as the prototype of classical Cepheid stars since the discovery of its variability by J. Goodricke in 1784 (Goodricke 1786, although the very first discovered Cepheid was  $\eta$  Aql, identified by E. Piggot a few months earlier).  $\delta$  Cep has therefore a particular historical interest as being the Cepheid archetype, and is also an important calibrator for the period–luminosity relation with the most accurate parallax for a Milky Way Cepheid ( $272 \pm 11$  pc; Benedict et al. 2002).  $\delta$  Cep is also a member of a star cluster (Majaess, Turner & Gieren 2012), and its very precise distance de-

rived from cluster membership confirms the parallax distance with a comparable uncertainty (4 per cent). Both distance determinations further show excellent agreement with the value derived by Storm et al. (2011) using the infrared surface brightness technique.

This 5.37 d pulsating star, which is also the second nearest Cepheid, has been extensively studied with several observing techniques and wavelengths, revealing little by little new unseen physical properties.  $\delta$  Cep is known to have an A0-type visual companion located at about 40 arcsec (Fernie 1966; Prugniel et al. 2007), which turns out to have itself an astrometric component (Benedict et al. 2002). The  $\delta$  Cep system is also associated with a circumstellar infrared nebulae, reminiscent of a bow shock aligned with the direction of the proper motion of the stars. This might have been created by the interaction between the stellar wind and the local

\*E-mail: [agallenn@eso.org](mailto:agallenn@eso.org)

**Table 1.** Journal of the observations.  $N_{V^2}$  and  $N_{CP}$ : number of squared visibilities and closure phases.

UT	MJD	$N_{V^2}, N_{CP}$	Configuration
2015 Jul. 31	57234.484	508, 379	S2-E1-E2-W1-W2
2015 Oct. 22	57317.313	303, 160	S2-E1-E2-W1-W2

interstellar medium, and might show that the Cepheid is losing mass (Marengo et al. 2010; Matthews et al. 2012).

Recently, from high-precision radial velocity measurements, Anderson et al. (2015) reported the detection of a spectroscopic companion, closer to the Cepheid than the visual component. They estimated an orbital period of about six years, and a projected semimajor axis of 21.2 mas ( $\sim 5.8$  au, assuming masses for the components). Evans (1992) set upper limits on any possible companions using IUE spectra, she excluded spectral types earlier than A3V ( $\sim 2.5 M_{\odot}$ ). Anderson et al. (2015) further pointed out that the companion mass is likely to be  $< 1.75 M_{\odot}$ . If the orbit is favourable and the contrast not too high between the components, the companion should be detected by interferometry. We therefore recently performed new and unique multitelescope interferometric observations with the MIRC instrument at the CHARA array (Center for High Angular Resolution Astronomy array), with the goal of detecting this companion. Our team has already proven that long-baseline interferometry is a powerful tool to spatially detect and resolve very close, faint companions orbiting classical Cepheids (Gallenne et al. 2013a,b, 2014, 2015).

## 2 CHARA/MIRC OBSERVATIONS AND DATA REDUCTION

The observations were performed in July and October 2015 using the Michigan InfraRed Combiner (MIRC) installed at the CHARA array (ten Brummelaar et al. 2005), located on Mount Wilson, California. The CHARA array consists of six 1 m aperture telescopes with a Y-shaped configuration (two telescopes on each branch), oriented to the east (E1, E2), west (W1, W2) and south (S1, S2), providing good coverage of the  $(u, v)$  plane. The baselines range from 34 to 331 m, providing a high angular resolution down to 0.5 mas in  $H$ . The MIRC instrument (Monnier et al. 2004, 2010) is an image-plane combiner which enables us to combine the light coming from all six telescopes in  $H$ . MIRC also offers three spectral resolutions ( $R = 42, 150$  and  $400$ ), which provide 15 visibility and 20 closure phase (CP) measurements across a range of spectral channels.

We observed  $\delta$  Cep (HD 213306, HIP 110991) with five telescopes (S2-E1-E2-W1-W2). We used the lowest spectral resolution, where the light is split into eight spectral channels. Table 1 lists the journal of our observations. We followed a standard procedure of observing a calibrator before and/or after our Cepheids to monitor the interferometric transfer function. The calibrators, HD 206349 ( $\theta_{UD} = 0.865 \pm 0.011$  mas) and HD 214454 ( $\theta_{UD} = 0.593 \pm 0.042$  mas), were selected using the `SEARCHCAL`<sup>1</sup> software (Bonneau et al. 2006) provided by the Jean-Marie Mariotti Center.<sup>2</sup>

The data were reduced using the standard MIRC pipeline (Monnier et al. 2007), which consists of computing the squared visibilities and triple products for each baseline and spectral channel, and to correct for photon and readout noises. Squared visibilities are

estimated using Fourier transforms, while the triple products are evaluated from the amplitudes and phases between three baselines forming a closed triangle. We then did an incoherent average of 30 s for the final data such that the projected baselines do not change significantly during one exposure, therefore reducing smearing of the CPs and optimizing the companion detection sensitivity.

## 3 COMPANION SEARCH AND SENSITIVITY LIMIT

To search for companion we used the tool CANDID<sup>3</sup> (Gallenne et al. 2015), made for this purpose. It allows a systematic search for companions performing an  $N \times N$  grid of fit, whose minimum needed grid resolution is estimated a posteriori. The tool delivers the binary parameters, namely the flux ratio  $f$  and the astrometric separation  $(\Delta\alpha, \Delta\delta)$ , but also the uniform disc angular diameter of the primary  $\theta_{UD}$ , and the (non-)detection level of the component. It uses  $\chi^2$  statistics to estimate the level of detection in ‘number of sigmas’, and therefore assumes the error bars are uncorrelated. We will claim a detection if the level is  $> 3\sigma$ .

We first CANDID for each individual data set (i.e. July and October) and searched around 100 mas from the Cepheid. We chose this limit because companions at larger distances are strongly impacted by the bandwidth smearing effect, and in addition are more efficiently detected using adaptive optics on a single-dish telescope (through imaging or sparse aperture masking). The first data set (July) gives a best fit at a detection level of  $2.5\sigma$  using all interferometric observables (i.e. the squared visibilities  $V^2$ , the closure phases CPs, and the bispectrum amplitudes), and  $3\sigma$  only using CPs. Fig. 1 shows the  $\chi_r^2$  map with the most probable location of a companion, if any, and the  $n\sigma$  map giving the detection level at each point in the grid for the July observations. A companion might be detected at  $\rho \sim 5$  mas and PA  $\sim -0.8^\circ$ , with a flux ratio of  $f \sim 0.21$  per cent, but other positions seem also possible with similar detection levels. Furthermore, such a flux ratio is below the average sensitivity limit reachable by the current beam combiners, but two components were already detected with such a contrast (Gallenne et al. 2015; Roettenbacher et al. 2015). The second data set (October) gives a best fit at a detection level of  $3.1\sigma$  both for all observables and only the CPs, but at distinct locations and very different flux ratios. As this second observation was performed under poor seeing conditions, the visibilities are probably biased and not reliable to detect such faint companions. With the CP only, the most probable location is at  $\rho \sim 7$  mas and PA  $\sim 2^\circ$ , and seems consistent with the July observations. However, the estimated flux ratio is 0.88 per cent, very different to 0.21 per cent in July. The magnitude difference of the Cepheid between the two phases is  $\sim +0.03$  mag (see Fig. 4), which would correspond to an  $\sim -3$  per cent change in flux ratio, and not a factor of 4. We therefore conclude that we do not have a detection in October, while it is marginal for July and just at our chosen detection threshold.

CANDID has also implemented a robust method to derive the dynamic range we can reach with a given set of data. It consist of injecting a fake companion into the data at each astrometric position with different flux ratios. As we inject a companion, we therefore know that the binary model should be the true model. We then compare the  $\chi^2$  with the one of a single star model (uniform disc model) to obtain the probability of the binary model to be the true model. We set the significance level on the flux ratios at

<sup>1</sup> Available at <http://www.jmmc.fr/searchcal>.

<sup>2</sup> <http://www.jmmc.fr>

<sup>3</sup> Available at <https://github.com/amerand/CANDID>.

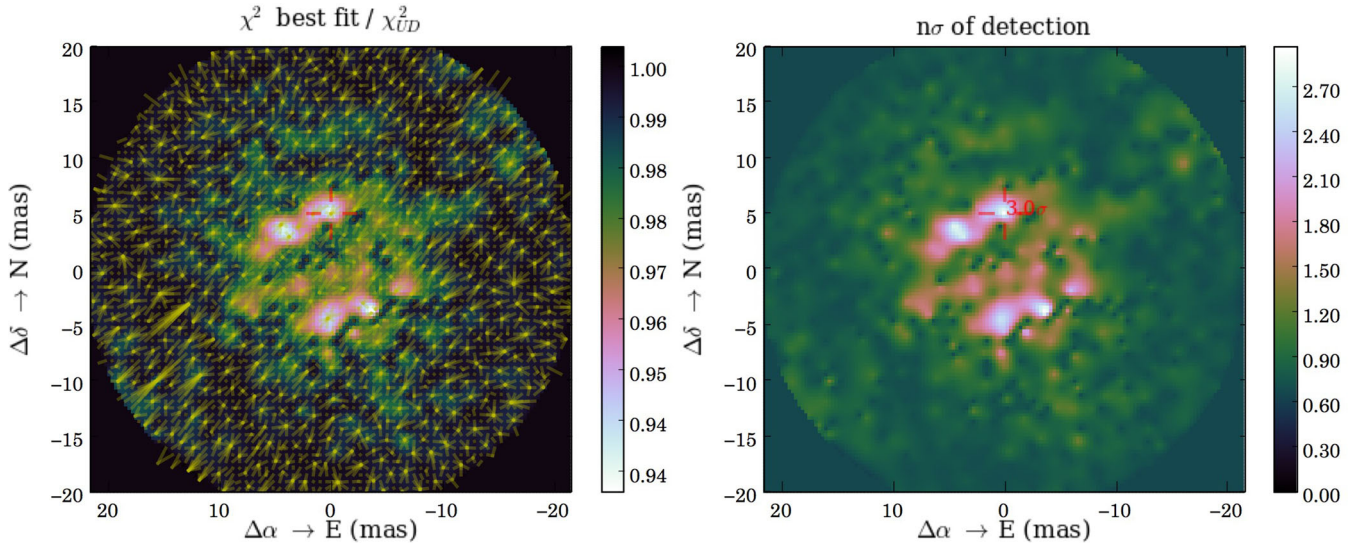


**Figure 1.**  $\chi_r^2$  map of the local minima (left) and detection level map (right) of  $\delta$  Cep using only the CP for the observations made in 2015 July. The yellow lines represent the convergence from the starting points to the final fitted position (for more details see Gallenne et al. 2015). The maps were re-interpolated in a regular grid for clarity.

**Table 2.**  $3\sigma$  contrast limits  $\Delta m$  of the companion in the  $H$  band. The relative distance  $r$  is expressed in mas. #1 and #2 denote the July and October observations, respectively.

	All Observables				Only CP			Sp. type limit		
	$r < 25$	$25 < r < 50$	$50 < r < 100$	$r < 25$	$25 < r < 50$	$50 < r < 100$	$r < 25$	$25 < r < 50$	$50 < r < 100$	
#1	6.17	5.63	5.26	6.44	5.82	5.24	F0V	A1V	B9V	
#2	4.24	3.68	3.51	4.35	3.45	2.88	B6V	B3V	B1V	

$3\sigma$ , meaning that lower flux ratios are not significantly detected. We refer the reader to Gallenne et al. (2015) for more information about the method. For comparison, CANDID has also implemented a less robust method which consist of comparing a uniform disc model with a binary model for each position in the grid, and then check whether the probability of the binary model is consistent with the data (Absil et al. 2011). In the following, all of the given detection limits are derived from our injection method, because we demonstrated in Gallenne et al. (2015) that the Absil’s method may under- or overestimate the detection limits.

We listed in Table 2 two detection limits for each data set, one using all of the observables, and one using only the CPs. We also gave three different values, the average for  $r < 25$  mas,  $25 < r < 50$  mas and  $50 < r < 100$  mas, which can be relevant when the limit increases with the relative distance to the Cepheid,  $r$ . All of the final  $3\sigma$  contrast limits,  $\Delta m_{3\sigma}$  expressed in magnitude, are conservative as they correspond to the mean plus the standard deviation for the given radius range. We present in Fig. 2 the contrast limit curve, using all observables, for the observations performed in July.

From an evolutionary time-scale point of view, most of the companions should be stars close to the main sequence. We therefore set upper limits for the companion spectral type assuming it is on the main sequence, and based on their  $H$ -band luminosities. From our estimated reported limits, we can exclude the presence of a companion having a spectral type earlier than a F0V star within 25 mas, A1V star between 25 and 50 mas, and B9V star between 50 and 100 mas from  $\delta$  Cep (estimated using intrinsic colours from Cox 2000 and Ducati et al. 2001). This would correspond to a companion mass  $< 1.6 M_{\odot}$ ,  $< 2.7 M_{\odot}$ , and  $< 3.4 M_{\odot}$ , respectively (Cox 2000). From those limits, we can check the consistency with the

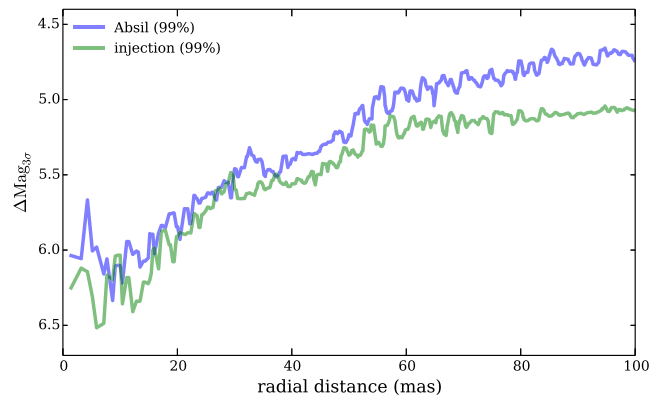


**Figure 2.** Contrast limit at  $3\sigma$ ,  $\Delta m_{3\sigma}$ , for a companion orbiting  $\delta$  Cep.

predicted orbit of Anderson et al. (2015). Using Kepler’s law and setting the projected separation  $r$  as a lower limit for the angular semimajor axis, that is  $a \geq r$ , we have

$$P^2 \geq \frac{r^3 d^3}{M_1 + M_2},$$

with  $r$  in arcsecond,  $d$  in parsec,  $P$  in year and the masses in solar mass. In Fig. 3, we plotted the function  $P_{\min}(r)$ , using a maximum Cepheid mass of  $6 M_{\odot}$  (see e.g. Matthews et al. 2012), and the previously cited mass limits for the companion. We also plotted the predicted upper-limit period (i.e.  $P + \sigma$ ) derived by Anderson et al. (2015). We can see that to be consistent with the expected period, the companion has to be located at  $r < 24$  mas, and has therefore

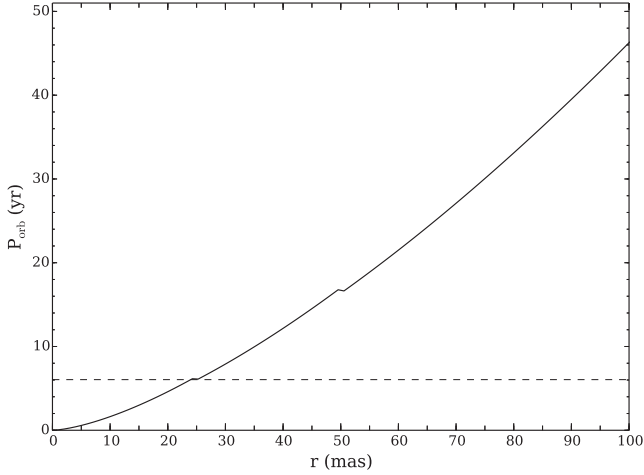


**Figure 3.** Minimum possible orbital period in function of the projected radial distance. The dashed line represents the period estimated from Anderson et al. (2015).

a spectral type later than an F0V star. It is also consistent with the predicted projected semimajor axis of 21.2 mas.

The marginally detected component with  $f = 0.21$  per cent ( $\Delta m = 6.7$  mag) would correspond to an F2V star, with a mass of about  $1.5 M_{\odot}$ , which would be consistent with the  $1.75 M_{\odot}$  upper limit pointed out by Anderson et al. (2015). The projected separation of  $\sim 5$  mas seems also consistent with our previous maximum separation threshold.

We can also set lower limit on the companion flux using the Cepheid  $H$ -band light curve from the literature, which would actually represent the combined flux in case of an unseen companion is present. We retrieved the photometry from Barnes et al. (1997) and used the ephemeris  $T_0 = 2448\ 305.236\ 2421$  d and  $P_{\text{puls}} = 5.366\ 2906$  d (Mérand et al. 2015) to construct the  $H$ -band light curve. To estimate the magnitudes at our given pulsation phases (i.e.  $\phi = 0.05$  and  $0.48$ ), we interpolated the data with a periodic cubic-spline function defined by floating nodes. The interpolated curve is shown in Fig. 4. We then estimated the combined magnitudes  $2.32 \pm 0.01$  mag and  $2.35 \pm 0.01$  mag, respectively, at phases  $\phi = 0.05$  and  $0.48$ . For simplicity and as those values are rather close, we used the averaged value and the standard deviation, giving the average combined magnitude  $m_{12} = 2.34 \pm 0.02$  mag. Following equation 2 of Gallenne et al. (2014),

$$m_2 = m_{12} + 2.5 \log(1 + 1/f), \quad (1)$$

with  $\Delta m = -2.5 \log f$ , and  $f$  the flux ratio between the companion and the Cepheid, we estimated a minimum  $H$ -band magnitude for the companion to be  $H_{\text{comp}} > 9.15, 8.31$  and  $7.77$  mag, respectively, for  $r < 25$  mas,  $25 < r < 50$  mas and  $50 < r < 100$  mas.

Another approach in deriving the luminosity class limit of this possible companion is to use the Hertzsprung–Russell (HR) diagram and our derived magnitude difference limits. We retrieved Geneva stellar isochrones (Ekström et al. 2012) for ages  $t = 95$ – $125$  Myr, a solar metallicity  $Z = 0.014$  and an initial rotation rate of  $\Omega/\Omega_{\text{crit}} = 0.568$ . Using the output of the isochrone models, i.e. effective temperatures and absolute magnitudes, we converted the  $L - T_{\text{eff}}$  HR diagram into a  $H$ -band absolute magnitude–temperature diagram ( $\Delta H - T_{\text{eff}}$ ) using the known properties of the Cepheid, i.e. the parallax  $\pi = 3.66 \pm 0.15$  mas (Benedict et al. 2002), an average effective temperature  $T_{\text{eff}} = 5900 \pm 100$  K (Andrievsky, Luck &

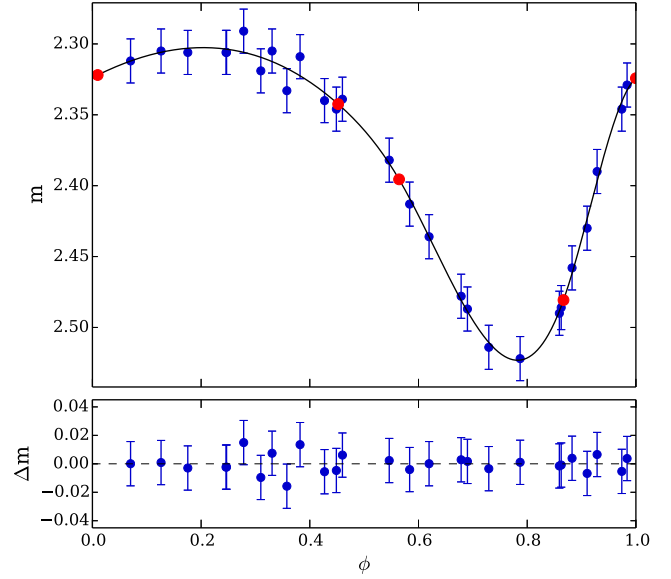


**Figure 4.**  $H$ -band light curve of  $\delta$  Cep. The solid line is the periodic cubic-spline function defined with five adjustable floating nodes (red dots).

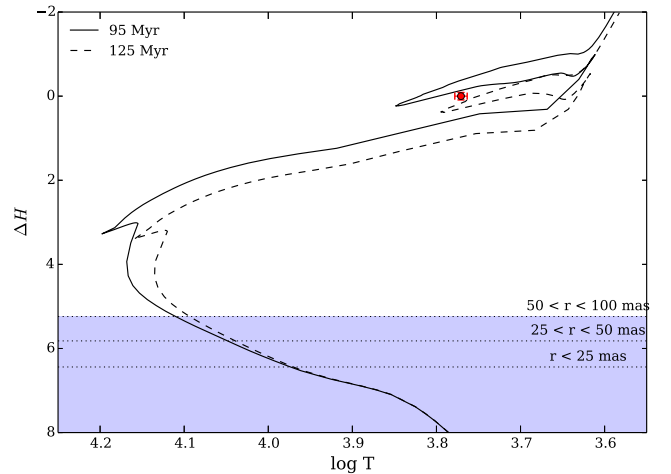


**Figure 5.** Isochrones from the Geneva evolution models (Ekström et al. 2012), normalized to the  $H$ -band absolute magnitude of the Cepheid. The red dot denotes the position of  $\delta$  Cep, while the dashed lines represent our derived magnitude limits. The blue area shows the possible luminosity class for an undetected companion.

Kovtyukh 2005), and an average apparent magnitude  $m_H = 2.38 \pm 0.01$  mag (Barnes et al. 1997). In Fig. 5, we show two isochrones encompassing the Cepheid properties (red dot). We see that the two isochrone limits give the same luminosity class limit for an undetected component, as indicated by the blue area in the figure, i.e. if a companion is orbiting  $\delta$  Cep, it should be a main-sequence or white dwarf star. The presence of a white-dwarf companion is not unlikely. This is possible if the companion was originally more massive than the Cepheid, but no white dwarf companion to a Cepheid has been found so far.

#### 4 ANGULAR DIAMETER

Our observations also provide measurements of the angular diameter of the Cepheid for two pulsation phases. We estimated the limb-darkened (Rosseland) diameter of the star following the

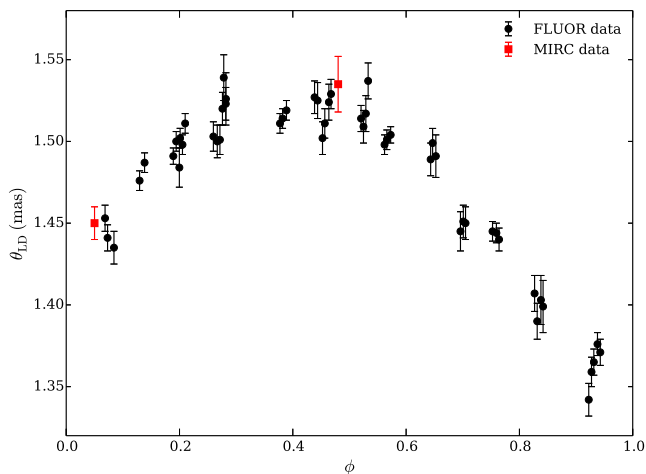


Figure 6. Limb-darkened disc angular diameter variation of  $\delta$  Cep.

formalism of (Mérand et al. 2015), i.e. we extracted the radial intensity profile  $I(r)$  of the spherical SATLAS models (spherical version of the ATLAS code, Neilson & Lester 2013, for temperatures of 6900 K and 5600 K at phases 0.05 and 0.048), which was converted to a visibility profile using a Hankel transform and fitted to our squared visibility data.

We measured  $\theta_{LD} = 1.450 \pm 0.010$  mas and  $\theta_{LD} = 1.535 \pm 0.017$  mas, respectively, at pulsation phases 0.05 and 0.48. These values have been estimated using the bootstrapping technique (with replacement) on all baselines. We took from the distributions the median, and the maximum value between the 16th and 84th percentiles as uncertainty. These measurements are in good agreement with the angular diameter variation curve previously reported with the instrument CHARA/FLUOR (Mérand et al. 2005, 2015), as shown in Fig. 6.

## 5 CONCLUSION

We reported new and unique multitelescope interferometric observations of the classical Cepheid  $\delta$  Cep. The goal was to detect the newly discovered spectroscopic companion reported by Anderson et al. (2015).

Our observations did not show strong evidence of any companion with a spectral type earlier than F0V, A1V and B9V, respectively, within the relative distance from  $\delta$  Cep  $r < 25$  mas,  $25 < r < 50$  mas and  $50 < r < 100$  mas. The spectral type limits are tighter than previous works for  $r < 25$  mas. We also estimated lower limit magnitudes for the companion to be  $H_{comp} > 9.15$ , 8.31 and 7.77 mag, respectively. We also showed that to be consistent with the predicted orbital period, the companion has to be located at a projected separation  $< 24$  mas and have spectral type later than an F0V star.

A component might have been marginally detected at only  $3\sigma$ , but we found several possible locations. Although the estimated flux ratio and separation are consistent with what expected, the detection is not really convincing. Additional data are necessary to claim a detection.

The regular dynamic range reachable by the current beam combiners is about 5.8 mag (200:1), making this new possible companion of  $\delta$  Cep hardly detectable from long-baseline interferometry, but not impossible as already demonstrated by Gallenne et al. (2015) and Roettenbacher et al. (2015), who detected components with a flux ratio of about 6.5 mag.

## ACKNOWLEDGEMENTS

The authors would like to thank the CHARA Array and Mount Wilson Observatory staffs for their support. This work is based upon observations obtained with the GSU Center for High Angular Resolution Astronomy Array at Mount Wilson Observatory. The CHARA Array is supported by the NSF under Grants No. AST-1211929 and AST-1411654. Institutional support has been provided from the GSU College of Arts and Sciences and the GSU Office of the Vice President for Research and Economic Development. JDM’s contribution to this work was partially supported by HST Guest Observer grants (HST-GO-13454.07-A, HST-GO-13841.006-A) and NSF (NSF-AST1108963). WG and GP gratefully acknowledge financial support for this work from the BASAL Centro de Astrofísica y Tecnologías Afines (CATA) PFB-06/2007. Support from the Polish National Science Centre grants MAESTRO DEC-2012/06/A/ST9/00269 is also acknowledged. PK, AG and WG acknowledge support of the French–Chilean exchange program ECOS-Sud/CONICYT (C13U01). The authors acknowledge the support of the French Agence Nationale de la Recherche (ANR), under grant ANR-15-CE31-0012-01 (project UnlockCepheids). RIA acknowledges funding from the Swiss National Science Foundation. WG also acknowledges financial support from the Millennium Institute of Astrophysics (MAS) of the Iniciativa Científica Milenio del Ministerio de Economía, Fomento y Turismo de Chile, project IC120009. This research received the support of PHASE, the high angular resolution partnership between ONERA, Observatoire de Paris, CNRS and University Denis Diderot Paris 7. This work made use of the SIMBAD and VIZIER astrophysical data base from CDS, Strasbourg, France and the bibliographic informations from the NASA Astrophysics Data System. This research has made use of the Jean-Marie Mariotti Center SearchCal and ASPRO services, co-developed by FIZEAU and LAOG/IPAG, and of CDS Astronomical Databases SIMBAD and VIZIER.

## REFERENCES

- Absil O. et al., 2011, *A&A*, 535, A68  
 Anderson R. I., Sahlmann J., Holl B., Eyer L., Palaversa L., Mowlavi N., Süveges M., Roelens M., 2015, *ApJ*, 804, 144  
 Andrievsky S. M., Luck R. E., Kovtyukh V. V., 2005, *AJ*, 130, 1880  
 Barnes T. G., III, Fernley J. A., Frueh M. L., Navas J. G., Moffett T. J., Skillen I., 1997, *PASP*, 109, 645  
 Benedict G. F. et al., 2002, *AJ*, 124, 1695  
 Bonneau D. et al., 2006, *A&A*, 456, 789  
 Cox A. N., 2000, *Allen’s Astrophysical Quantities*. Am. Inst. Phys., New York  
 Ducati J. R., Bevilacqua C. M., Rembold S. B., Ribeiro D., 2001, *ApJ*, 558, 309  
 Ekström S. et al., 2012, *A&A*, 537, A146  
 Evans N. R., 1992, *ApJ*, 384, 220  
 Fernie J. D., 1966, *AJ*, 71, 119  
 Gallenne A., Kervella P., Mérand A., Monnier J. D., Breifelder J., Pietrzyński G., Gieren W., 2013a, in Pavlovski K. Tkachenko A., Torres G., eds, *EAS Publ. Ser. Vol. 64, Setting a New Standard in the Analysis of Binary Stars*. p. 197  
 Gallenne A. et al., 2013b, *A&A*, 552, A21  
 Gallenne A. et al., 2014, *A&A*, 561, L3  
 Gallenne A. et al., 2015, *A&A*, 579, A68  
 Goodricke J., 1786, *Roy. Soc. London Philos. Trans. Ser. I*, 76, 48  
 Majaess D., Turner D., Gieren W., 2012, *ApJ*, 747, 145  
 Marengo M. et al., 2010, *ApJ*, 725, 2392  
 Matthews L. D., Marengo M., Evans N. R., Bono G., 2012, *ApJ*, 744, 53

- Mérand A. et al., 2005, *A&A*, 438, L9  
Mérand A. et al., 2015, *A&A*, 584, A80  
Monnier J. D., Berger J.-P., Millan-Gabet R., ten Brummelaar T. A., 2004, in Traub W. A., ed., *Proc. SPIE Conf. Ser. Vol. 5491, New Frontiers in Stellar Interferometry*. SPIE, Bellingham, p. 1370  
Monnier J. D. et al., 2007, *Science*, 317, 342  
Monnier J. D. et al., 2010, in Danchi W. C., Delplancke F., Rajagopal J. K., eds, *Proc. SPIE Conf. Ser. Vol. 7734, Optical and Infrared Interferometry II*. SPIE, Bellingham, p. 77340G  
Neilson H. R., Lester J. B., 2013, *A&A*, 556, A86  
Prugniel P., Soubiran C., Koleva M., Le Borgne D., 2007, *VizieR Online Data Catalog*, 3251, 0  
Roettenbacher R. M. et al., 2015, *ApJ*, 809, 159  
Storm J. et al., 2011, *A&A*, 534, A94  
ten Brummelaar T. A. et al., 2005, *ApJ*, 628, 453

This paper has been typeset from a  $\text{\TeX}/\text{\LaTeX}$  file prepared by the author.